

國立臺灣大學電機資訊學院資訊工程學研究所

碩士論文

Department of Computer Science and Information Engineering

College of Electrical Engineering and Computer Science

National Taiwan University

Master Thesis

基於內容認知實現影像去霧化

A Content Aware Method for Single Image Dehazing



Chao-Tsung Chu

指導教授：李明穗 博士

Advisor: Ming-Sui Lee, Ph.D.

中華民國 98 年 7 月

July, 2009

誌謝

能完成本篇論文，首先我要特別感謝我的指導教授，李明穗老師，我在李老師身上學到的不只是專業知識，更重要的是待人處世以及解決問題該有的方法與態度。接著感謝我的口試委員，吳家麟教授、郭天穎教授、葉家宏教授，感謝你們在口試時提醒我的不足之處，以及讓我深入思考研究上沒注意到的問題，使本論文得以更加完善。

此外我要感謝這個實驗室的同仁，包含了許多同學與學弟妹。感謝我的實驗室同學好夥伴，鈞哥(劉鴻鈞)、小瑋(張宸瑋)、吉米(謝若元)、鈺翔(邱鈺翔)，我們一起經歷了這兩年研究與修課的歲月。還有還在的實驗室學弟妹，小咖(陳美庭)、永青(張永青)、尾鰭(陳韋麒)、逸民(楊逸民)。在研究之餘，大家還常常聚在一起打球運動，保持健康的生活。因為有你們在實驗室的幫忙與討論，我才能把這篇論文完成。

還有我要感謝提供我在生活以及求學上補助的人及單位，學校及實驗室在我的碩士生活提供我定期的補助，讓我減輕在外租屋生活的壓力。多位家教的家長也惠我良多，我要感謝的人真的是太多了。接著，我要感謝我的家人，感謝我的父母，讓我每次回家時總有溫暖的感覺，有時因為壓力而在家庭產生負面的情緒，想想我真不是一個好孩子，總讓你們包容我；感謝柯爸爸、柯媽媽與柯姐姐在求學路上一直給予我支持，也給我很多意見與幫助；也感謝我的妹妹，在一同出外求學時有了個伴。

最後，我要感謝一個最重要的人，宜均(柯宜均)，從大學到研究所，一共陪我經歷了近三年的歲月。在這段日子，我們一起成長、一起歡笑、一起難過，不論發生什麼大大小小的事情，你總是陪在我身邊。感謝妳這三年的陪伴，因為有妳在，讓我安心地朝自己的目標前進，因為有妳，讓我在人生感到徬徨時而變得積極，也在我全心研究時，依然陪在我的身邊。希望我們能一直一直走下去，在未來的日子也能互相扶持與成長，更加懂得愛與珍惜。

中文摘要

在這本篇論文中，我們提出一個基於適性內容實現單張影像去霧化的方法。由於影像被霧化的程度與距離息息相關，而對於一張影像，每個特定區域(例如：樹、建築物或其他物體)裡面的像素，到相機的距離大致上都會一樣，所以我們假設每個區域被霧化的程度也會相同。在這樣的假設下，我們發展出一個對影像去霧化的方法。

首先，我們用暗原色先驗統計(Dark Channel Prior)的方法來預估霧光 (airlight) 的值。霧光(airlight)是在一張霧化的照片中用以代表霧的元素。基於我們觀察到在一張影像中，一個特定區域的像素裡面的像素，到相機的距離大致上都會一樣，所以每個區域的霧化轉換 (transmission) 值會是一樣的。所以我們用基於平均值移動分割(Mean Shift segmentation) 的方法分割我們的輸入影像。接著，我們使用一個函數來預估每一個區域的霧化轉換。預估完霧化轉換之後，我們用 Soft Matting 的方法把我們原先預估的霧化轉換對應圖變的更好。然後把霧化的影像給回復回來。實驗結果顯示出我們提出的方法，可以有效地對影像實現去霧，並且提供了一個準確預估的霧化轉換之值可以作為更深入的應用。

關鍵字：單一影像去霧化、基於平均值移動分割(Mean Shift segmentation)、暗原色先驗統計(Dark Channel Prior)、Soft Matting、影像回復

ABSTRACT

In this thesis, we present a content adaptive method for single image dehazing. Since the degradation level affected by haze is related to the depth of the scene and pixels in each specific part of the image (such as trees, buildings or other object) tend to have same depth to the camera, we assume that the degradation level affected by haze of each region is the same. Based on this assumption, we develop a single image dehazing method.

First, we use Dark Channel Prior method to estimate the airlight vector which represents the haze component in hazy images. By the observation that pixels in each specific part of the image (such as trees, buildings or other object) tend to have same depth to the camera, the transmission in this region is also the same. So, we use Mean Shift segmentation to segment our input image into different regions. Then, we recover the scene radiance by using a cost function estimating the transmission in each region. After the transmission map was estimated, we use Soft Matting to refine this transmission map. Results demonstrate the proposed method's power to remove the haze layer as well as provide a reliable transmission map which can be exploited for further usage.

Index Terms — Single Image Dehazing, Mean Shift segmentation, Dark Channel Prior, Soft Matting, Image Restoration

CONTENTS

口試委員會審定書	#
誌謝	i
中文摘要	ii
ABSTRACT	iii
CONTENTS	iv
LIST OF FIGURES	vi
Chapter 1 Introduction.....	1
1.1 Introduction of Dehazing.....	1
1.2 Thesis Organization.....	3
Chapter 2 Related Work.....	5
2.1 Haze Degradation Model Overview	5
2.2 Related Work of Dehazing.....	6
2.2.1 Dark Channel Prior	7
2.2.2 Correction of Contrast Loss	8
2.2.3 Single Image Dehazing Methods	9
2.2.4 Multiple Image Dehazing Methods.....	11
2.2.5 Dehazing Methods with User Input	12
2.3 Mean Shift Segmentation	13
2.4 Soft Matting.....	14
Chapter 3 Single Image Dehazing using Mean Shift Segmentation.....	16
3.1 System Overview.....	16
3.2 Image Segmentation	17

3.3	Atmospheric light Estimation.....	19
3.4	Cost Function for Transmission Map Estimation.....	21
3.5	Refinement of Transmission Map using Soft Matting.....	25
3.6	Recovering the Scene Radiance	27
Chapter 4	Experimental Results.....	29
4.1	Resultant images.....	29
4.2	Comparison with other haze removal methods	41
Chapter 5	Conclusion and Future Work.....	45
5.1	Conclusions	45
5.2	Future work.....	46
REFERENCE	50



LIST OF FIGURES

Fig. 1.1	A hazy image and its corresponding dehazed result.	3
Fig. 2.1	Failure case of dark channel method.....	8
Fig. 3.1	The flowchart of our proposed method.....	17
Fig. 3.2	A resultant image after applying mean shift segmentation.	19
Fig. 3.3	An image shows the difference between the-highest-intensity-pixel method and dark channel method.....	21
Fig. 3.4	The transmission map estimated by the cost function.....	25
Fig. 3.5	The transmission map after refinement using soft matting.....	27
Fig. 3.6	The resultant image after applying our proposed algorithm.	28
Fig. 4.1	A resultant image of our proposed haze removal method.....	32
Fig. 4.2	A resultant image of our proposed haze removal method.....	33
Fig. 4.3	A resultant image of our proposed haze removal method.....	34
Fig. 4.4	A resultant image of our proposed haze removal method.....	35
Fig. 4.5	Dehazing using the transmission map without refinement.	36
Fig. 4.6	The resultant image from the image taken by ourselves.....	37
Fig. 4.7	The resultant image from the image taken by ourselves.....	38
Fig. 4.8	The resultant image from the image taken by ourselves.....	39
Fig. 4.9	The resultant image from the image taken by ourselves.....	40
Fig. 4.10	Comparison with Tan's work [12].....	42
Fig. 4.11	Comparison with Dark Channel Prior method [13].	43
Fig. 4.12	Comparison with Fattal's work [2].	44
Fig. 5.1	Failure case. The image contains too much sky portion.	48

Fig. 5.2 Failure case from the image taken by ourselves.49



Chapter 1 Introduction

While taking pictures from outdoor scene, sometimes fog or haze appears in our images. This circumstance is caused by the presence of aerosols like dust and mist which forces the light to turn into another direction of propagation. This effect blocks the image details so that we cannot get sufficient information in the hazy part of the image. Thus, we may want to eliminate this kind of effect to get a haze-free image.

1.1 Introduction of Dehazing

Haze is an annoying factor when it shows up in the image since it causes poor visibility. This is the major problem of some applications in the field of computer vision, such as surveillance, object recognition, etc. In order to obtain the clear images, haze removal is inevitable.

Fog, haze and some other particles that degrade the scene image are the results of atmospheric absorption and light scattering. The radiance achieved to camera along the sight-line is decreased due to atmospheric light and it is replaced by previously scattered light, which is called the airlight. This degradation will cause the image to lose contrast and color correctness. Furthermore, the airlight which affect the image depends on the depth of the scene. This knowledge is commonly used for dehazing problems. We also adopt this clue to solve the haze removal problem.

Image haze removal has gotten a growing interest recently. More and more methods are introduced in the past three years. Nevertheless, dehazing is a challenging topic since the haze is dependent on the unknown depth information. Many different kinds of methods were proposed including single image dehazing methods, multiple image dehazing methods and methods with user's input. More details are discussed in the next chapter.

A haze free image is often preferred in many applications such as feature detection, photometric analysis and some other vision problems. Some aerial images taken by satellite may have to adopt this algorithm to get a lucid image for further usage. We may use this dehazing technique to help the car drivers to get a clearer view of path to avoid car accidents.

In order to obtain the clear image mentioned above, a haze removal method is proposed. A brief overview of our method is described as follows. First, we segment the image obtained from a hazy scene by mean shift segmentation. By the clue that each image segment has approximately the same depth, a cost function is exploited for estimating the airlight or the transmission. The transmission is the amount of the light that is not scattered and received by the camera. And we use a soft matting technique to refine our transmission map. Finally, this refined transmission map is exploited to recover the scene radiance. Figure 1.1 shows a hazy image and its dehazed result. We

can see the resultant image is clearer than the input image.

Our proposed method is based on the observation that pixels in each segmented region have the same depth. Each region is treated as a different object, and a cost function is exploited in each region. It's the key of divide-and-conquer. Despite the challenge of single image dehazing, the proposed method successfully removes the haze in the image. So, we can get a clear and vivid image for further applications by our proposed method.



Fig. 1.1 A hazy image and its corresponding dehazed result.

(a) hazy input image. (b) resultant image.

1.2 Thesis Organization

The organization of the thesis is as follows. We begin by reviewing previous works on image segmentation, haze removal and image matting in chapter 2. In chapter 3, the

core idea of our proposed method is presented and the details of the proposed method are explained. Then, the experimental results are reported in chapter 4. Also, some comparisons with alternative methods are also demonstrated in this chapter. At last, we summarize our approach and future work in chapter 5.



Chapter 2 Related Work

In the field of computational photography, there has a gain of focus on developing methods that recover hazy images at minimal requirements such as input data, user intervention, and elaborateness of the acquisition hardware. Image haze-removal is a very challenging and sophisticating problem to deal with. It is an ill-posed problem as we can see from the image degradation model.

Methods and algorithms for image dehazing are widely proposed. We introduce these methods in the following subsection. We also discuss about image segmentation algorithms such as mean shift algorithm. Image matting approach is reported as well.

2.1 Haze Degradation Model Overview

The haze image degradation model is described in this subsection. The following equation is widely used to describe the formation of a hazy image:

$$\mathbf{I}(x) = \mathbf{J}(x)t(x) + \mathbf{A}(1 - t(x)),$$

where $\mathbf{I}(x)$ is the input image at pixel x , \mathbf{J} is the scene radiance or the desired haze-free image. \mathbf{A} is the atmospheric light vector, which replaces the light processing from the scene by scattering. t is the medium transmission which is used to describe the portion of the light that is not scattered and received by the camera. The target of haze removal

is to recover J by two unknown factor t and A and the input image I .

In this degradation model, we can see two terms: $\mathbf{J}(x)t(x)$ and $\mathbf{A}(1 - t(x))$. The first term is called the direct attenuation[2][8][9][12][13]. It is used to describe the scene radiance and the level it declines in the medium. The second term is sometimes called airlight [2][8][9][12][13]. This term is describing the degree of substitution of the atmospheric light for the original light from the scene. The transmission t in this equation is describing the portion of the light that is not scattered and received by the camera. It is widely expressed by the following equation,

$$t(x) = e^{-\beta d(x)}.$$

β is the medium extinction coefficient due to light scattering. It is assumed to be a constant while the atmospheric light is homogeneous and $d(x)$ is the distance from the object to the camera at pixel x . We can clearly see that the transmission t totally depends on the depth d . The transmission is necessary while recovering the scene radiance. This is the challenging part of image dehazing. Once we get the transmission map, we can also get the depth map as a byproduct.

2.2 Related Work of Dehazing

First, we talk about two methods that affect our method the most, Dark Channel Prior method[13] and Correction of Contrast Loss[14]. Then, we arrange the rest of the

dehazing methods into single image dehazing methods, multiple image dehazing methods and dehazing methods with user interventions besides these two methods.

2.2.1 Dark Channel Prior

Dark Channel Prior method is a recently proposed method [13]. They introduced a strong prior called dark channel prior. This prior is based on the observation that at least one color channel has a low intensity value at some pixels of non-sky patches in haze-free outdoor images. They called this low-intensity channel the dark channel. This kind of low intensities is caused by three factors: shadows, colorful objects or surfaces and dark objects or surfaces. They used this powerful dark channel prior to estimate the transmission map and the atmospheric light.

They first used the dark channel prior to estimate the atmospheric light. Then, they derived the transmission map by the assumption that the dark channel of the haze-free image J tend to be 0. After estimating the transmission map, they used the soft matting technique to refine it. We also adopt this great technique to refine our transmission map. According to the refined transmission map, they can get the final dehazed image.

Unlike other haze removal methods, they proposed a powerful and strong prior – the dark channel prior – to solve image dehazing problem. The results applying their method seem to be good and satisfiable. Although, their method still exists some

limitations. In Fig. 2.1 we can see that their method underestimate the transmission of the white marble. This is because the scene objects are inherently similar to the atmospheric light and no shadow is cast on them. When this situation occurs, the dark channel prior is invalid.



Fig. 2.1 Failure case of dark channel method.

Left: input image. Middle: dehazed image. Right: the transmission map.

The transmission map of the marble is underestimated.

2.2.2 Correction of Contrast Loss

This method is proposed by [14]. They proposed an algorithm to estimate the level of airlight given the assumption that it is constant throughout the image. The airlight is referred to the second component of the haze image degradation model, $\mathbf{A}(1 - t(x))$.

The core idea of this method is based on a cost function. The cost function they

presented is as follows:

$$S(\lambda) = \text{STD} \left\{ \frac{\rho'_k - \lambda}{\bar{\rho}'_k - \lambda} \right\} \cdot \text{GM} \{ \bar{\rho}'_k - \lambda \}.$$

STD means the standard deviation and GM means the geometric mean. λ is the estimated airlight, ρ'_k is the hazy pixel value at pixel k and $\bar{\rho}'_k$ is the output of a spatial low-pass filter at pixel k . The objective is to get a λ to minimize the function and this λ is the airlight offset. We use their cost function to estimate the transmission of each region which is segmented by mean shift segmentation since transmission in each region is the same by our assumption.

2.2.3 Single Image Dehazing Methods

Dehazing methods using single input image have been proposed more than methods using multiple input images. Experts are more focusing on methods for single image dehazing. In this subsection, we discuss about the methods for single image dehazing.

In Fattal's work [2], they present a method to estimate the optical transmission in hazy scenes given a single input image. This approach relies only on the assumption that the transmission and surface shading are locally uncorrelated. They can also provide reliable transmission estimation. Based on the recovered transmission values they can estimate scene depths and use them for other applications such as image

refocusing and novel view synthesis.

In Tan's method [12], they present an automated method that only requires one single input image to solve the problem that bad weather degrades visibility. Their method is based on two basic observations: first, images with enhanced visibility (or clear-day images) have more contrast than images plagued by bad weather; second, airlight, whose variation mainly depends on the distance of the objects to the viewers, tends to be smooth. By using these two observations, they develop a cost function in the framework of Markov random fields, which can be efficiently optimized by various techniques, such as graph-cuts or belief propagation. Then, they solve the optimization problem to remove haze from the input image.

In [16], they present a new algorithm FSSR (Fast Single-Scale Retinex) for defogging topic, which is based on SSR (Single-Scale Retinex) algorithm. A good enhance results for foggy SSR algorithm has been gotten by using SSR algorithm. But huge computation must be applied since for every pixel, a convolution has to be computed. So, they present an approved SSR algorithm to reduce the computation cost.

In [17], they propose an effective method to correct the degraded image by subtracting the estimated airlight map from the degraded image. Airlight can be estimated using a cost function that is based on the human visual model, wherein a human is more insensitive to variations of the luminance in bright regions than in dark

regions.

2.2.4 Multiple Image Dehazing Methods

Yoav's work [10] is based on the polarization difference of a hazy scene image. They use the polarizer to take images with different degrees of polarization in order to execute the dehazing method. They are totally physics-based, but they have to take several images of the same scene. We only have to use one single image which is the minimal input.

Yoav [11] introduces a new method for blindly recovering the airlight, thus recovering contrast, with neither user interaction nor existence of the sky in the frame after [10]. Their method blindly separates the airlight radiance (the main cause for contrast degradation) from the objects signal. It works even if no sky exists in the FOV (field of view). The method exploits mathematical tools developed in the field of blind source separation (BSS), also known as independent component analysis (ICA). They show that the radiance of haze (airlight) can be separated by ICA, by the use of a simple pre-process. And another important part of their method is that their method is physics-based, rather than being pure ICA of mathematically abstract signals. They use the observation that human vision can correct for effects of aerial perspective on the basis of context.

2.2.5 Dehazing Methods with User Input

In [8], they proposed three interactive algorithms to move weather effects. It is a clearer version of the algorithms they mentioned in [9]. The three algorithms they proposed are as follows: Dichromatic Color Transfer, Deweathering using Depth Heuristics and Restoration using Planar Depth Segments and Adding Weather Effects to Images.

In Dichromatic Color Transfer, they described an algorithm to transfer colors from nearby regions to replace colors of regions that are most effected by bad weather, in a physically consistent manner. This method requires two manual inputs: first, they select a nearby region in the image where colors are not corrupted (or, minimally altered) by bad weather and the second one they select is the region that most resembles the color of airlight.

In Deweathering using Depth Heuristics and Restoration using Planar Depth Segments, this is the most important section of their method. They use the same image model of foggy images and with two proper manual inputs to get a dehazed image. First, they input the approximate location of a vanishing point along the direction of increasing distance in the image. Next, they input the approximate minimum and maximum distances and interpolate distances (say, using a linear or quadratic function)

for points in between. By the selected vanishing point, they can calculate the distances of the scene points since they are inversely related to their image distances to the vanishing point.

In "Restoration using Planar Depth Segments", they observed some images with planar objects like building can do some specific moves to simplify the algorithm. That is, they provide a rough depth segmentation of the scene. Thus, planar depth segments should suffice for deweathering in urban scenes and the rest of the algorithm is basically the same as in Deweathering using Depth Heuristics.

This method requires user interventions to indicate where the unaffected region is and where the vanishing point is. When the user inputs wrong information, their method could easily fail. Our method doesn't encounter such problem since we automatically solve the dehazing problem without any kinds of user interventions.

2.3 Mean Shift Segmentation

In this subsection, we discuss about the image segmentation algorithm we used – Mean Shift Algorithm [15]. This general nonparametric technique is proposed for the analysis of a complex multimodal feature space and to delineate arbitrarily shaped clusters in it. The basic computational module of the technique is an old pattern recognition procedure, the mean shift. They prove for discrete data the convergence of a

recursive mean shift procedure to the nearest stationary point of the underlying density function and, thus, its utility in detecting the modes of the density.

Algorithms for two low-level vision tasks, discontinuity preserving smoothing and image segmentation are described as applications. In these algorithms, the only user set parameter is the resolution of the analysis and either gray level or color images are accepted as input. The reason we use this segmentation method is that it is robust and the best method recently.

2.4 Soft Matting

From a computer vision perspective, soft matting is extremely challenging because it is massively ill-posed — at each pixel we must estimate the foreground and the background colors, as well as the foreground opacity (“alpha matte”) from a single color measurement. Current approaches either restrict the estimation to a small part of the image, estimating foreground and background colors based on nearby pixels where they are known, or perform iterative nonlinear estimation by alternating foreground and background color estimation with alpha estimation.

Levin [4] presents a closed form solution to natural image matting. They derive a cost function from local smoothness assumptions on foreground and background colors, and show that in the resulting expression it is possible to analytically eliminate the

foreground and background colors to obtain a quadratic cost function in alpha. This allows them to find the globally optimal alpha matte by solving a sparse linear system of equations. Furthermore, the closed form formula allows them to predict the properties of the solution by analyzing the eigenvectors of a sparse matrix, closely related to matrices used in spectral image segmentation algorithms.

This soft matting skill is very useful in dehazing since the alpha map in matting equation is similar with the transmission map in hazy image degradation model. With an appropriate adjustment, we can exploit this method to refine our transmission map.



Chapter 3 Single Image Dehazing using Mean Shift Segmentation

In this chapter, we propose our method for removing haze. We go through the whole system step by step. First, we introduce our method by a system overview. Then, we discuss the details in each step including how we segment the input image, how atmospheric light and transmission map is estimated.

3.1 System Overview

The proposed system is illustrated in Fig. 3.1. It contains 5 steps: Image Segmentation, Atmospheric light Estimation, Cost Function for Transmission Map Estimation, Refinement of Transmission Map using Soft Matting and Recovering the Scene Radiance.

For Image Segmentation, we use Mean Shift region segmentation algorithm [15] to segment the input image into different regions. Then, we estimate the atmospheric light using the method proposed by [13]. By observing the segmented image, we can see that each region of the image tends to have the same distance from camera to the scene of that region. This is the core idea of our proposed method. We split the input image into each distant-like region and try to deal with each small region at a time instead of

dealing with the whole image at a time. It's the spirit of divide-and-conquer.

Then, we use the algorithm proposed from [14] as the cost function for estimating the transmission map and apply Soft Matting Algorithm [4] to refine our estimated transmission map. Finally, we can get the desired haze-free image by recovering the scene radiance.

In the following subsections, we will discuss each step and explain why we use these algorithms more explicitly.

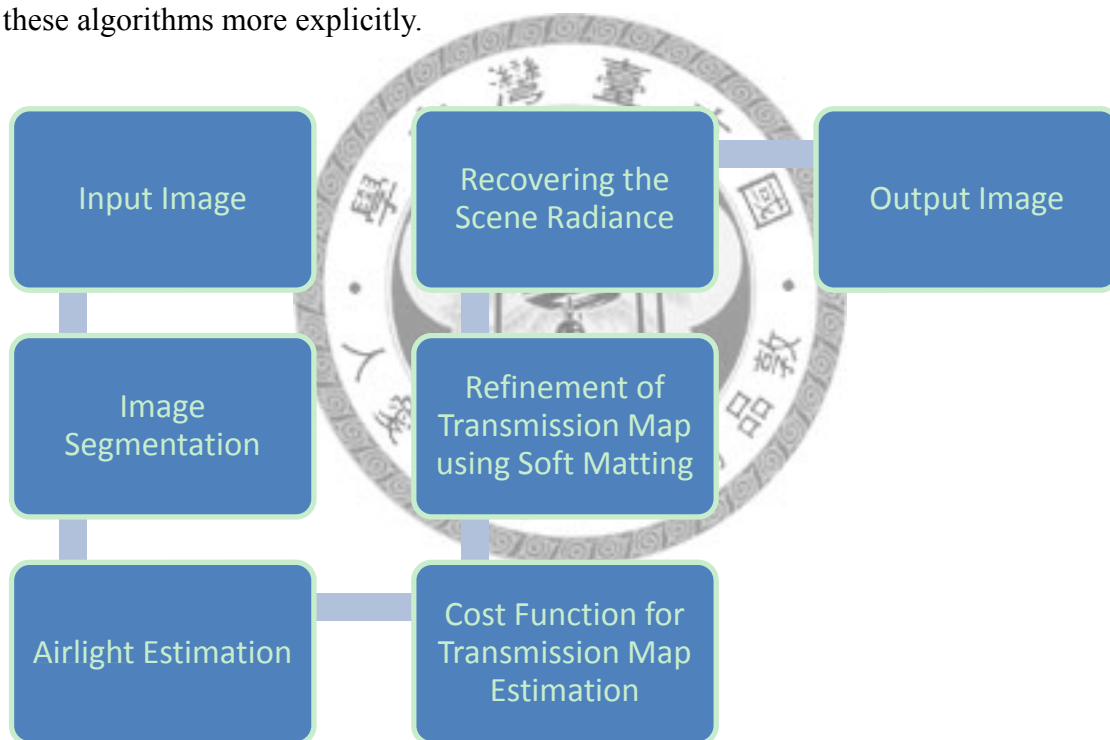


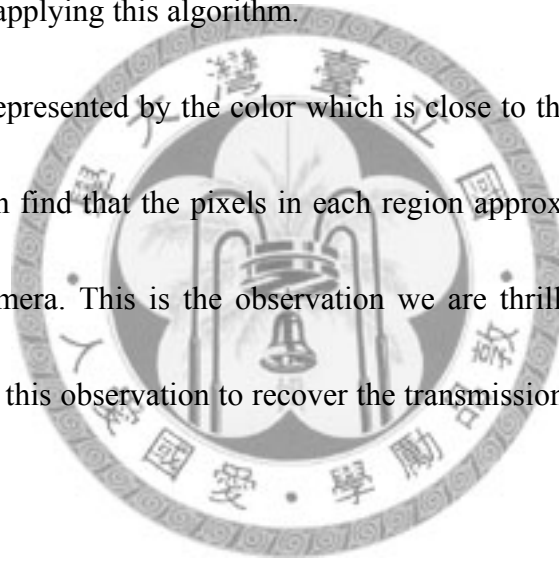
Fig. 3.1 The flowchart of our proposed method.

3.2 Image Segmentation

In this subsection, we discuss how we segment our input image. We use Mean

Shift algorithm to carry out this step. As we mentioned, this segmentation method is the most powerful method for region segmentation nowadays. Mean Shift is a robust segmentation method while comparing to other segmentation methods. The core technique of this algorithm – mean shift, is not originally used in this area. It was used for clustering before. Then, it is recollected and redirected toward this orientation. We apply this algorithm to do image segmentation and obtain a great result. Fig. 3.2 is a resultant image after applying this algorithm.

Each region is represented by the color which is close to the color appears mostly in this region. We can find that the pixels in each region approximately have the same distance from the camera. This is the observation we are thrilled about. After image segmentation, we use this observation to recover the transmission map in subsection 3.4 later.





(a)

(b)

Fig. 3.2 A resultant image after applying mean shift segmentation.

(a) Input image. (b) Segmented image.

3.3 Atmospheric light Estimation

When it comes to atmospheric light estimation, we have plenty of methods to estimate atmospheric light. In most of the haze removal algorithms, the atmospheric light A is estimated from the most haze-opaque pixel. For example, in [12], the atmospheric light is estimated by using the pixel with the highest intensity. But, the brightest pixel in an image may be a white object or come from a white object such as a white car or a white goose. We use a better method instead of using the highest intensity pixel to be our estimated atmospheric light.

As mentioned in 2.1.1, the dark channel prior method gives a great result. The dark

channel prior is a strong prior, they use it in their method even in the way they estimate atmospheric light. It turns out that using dark channel prior to estimate atmospheric light is more accurate than other methods and it is very easy to implement. So, we decide to use the method they proposed to estimate the atmospheric light.

First, we pick the top 0.1% brightest pixels in the dark channel image. The dark channel image is obtained by extracting the lowest intensity value of r, g and b channels in a mask over the input image. These pixels are most haze-opaque pixels. Then, we choose the pixel which has the highest intensity in the input image to be our atmospheric light. This selected pixel may not have the highest intensity in the input image. We show the different pixels being selected by these two simple methods in Fig. 3.3. Red circle is where the pixel picked using dark channel method located and yellow circle is where the highest intensity pixel located. As we can see, the dark channel prior method is more accurate than choosing the highest intensity method.



Fig. 3.3 An image shows the difference between the-highest-intensity-pixel method and dark channel method.

Red circle is using dark channel method. Yellow circle is the highest intensity pixel.



3.4 Cost Function for Transmission Map Estimation

After image segmentation and atmospheric light estimation, we have to figure out how to estimate the transmission map. We have an observation in subsection 3.2 that the distance from the camera to the scene in each region tends to be the same. So, according to the hazy image degradation model

$$\mathbf{I}(x) = \mathbf{J}(x)t(x) + \mathbf{A}(1 - t(x)), t(x) = \exp(-\beta d(x)),$$

the transmission $t(x)$ is the same in each region. This enables us to use a cost function

to estimate $t(x)$ in each region.

In Tan's method [12], they use an MRF model as their cost function for calculating transmission value t . Their method is not physically based and may underestimate the transmission. In Oakley's method [14], they first assume that the whole image is affected by the same level of airlight. It means that the transmission t is the same over the entire image. Then, they use the cost function they proposed to find the transmission t . We can apply Oakley's method into this step since the transmission in each region is also the same according to our assumption. We apply the cost function to each region at a time and find the transmission t of that region. Because their method is physically based and has a strict proof of validity, we get a physically based result unlike Tan's method.

Oakley and Bu mentioned two kinds of cost functions: multichannel cost function and multiscale optimization,

$$S_{mc}(\lambda_r, \lambda_g, \lambda_b) = \frac{1}{K} \sum_{p \in \{r, g, b\}} \sum_{k=1}^K \left(\frac{\rho_k^p - \bar{\rho}_k^p}{\bar{\rho}_k^p - \lambda_p} \right)^2 \cdot \exp \left\{ \frac{1}{3K} \sum_{p \in \{r, g, b\}} \sum_{k=1}^K \ln(\bar{\rho}_k^p - \lambda_p)^2 \right\},$$

$$S_{ms}(\lambda) = \frac{1}{K} \sum_{l=1}^L \sum_{k=1}^K \left(\frac{\bar{\rho}_k^{\sigma_{l,1}} - \bar{\rho}_k^{\sigma_{l,2}}}{\bar{\rho}_k^{\sigma_{l,2}} - \lambda} \right)^2 \cdot \exp \left\{ \frac{1}{L \cdot K} \sum_{l=1}^L \sum_{k=1}^K \ln(\bar{\rho}_k^{\sigma_{l,2}} - \lambda)^2 \right\}.$$

S_{mc} is the multichannel cost function and S_{ms} is the multiscale cost function. λ is the second term of the hazy image degradation model, $A(1 - t(x))$, which is called the airlight. ρ_k is the hazy pixel value at pixel k and $\bar{\rho}_k$ is the output of a spatial low-pass filter at pixel k . In multichannel optimization, they split the components λ , ρ_k , $\bar{\rho}_k$ into three channels and execute optimization. In multiscale optimization, $\sigma_{l,1}$ is referred to a base scale of spatial low-pass filter and $\sigma_{l,2}$ is $\sigma_{l,1}$ add to a scale difference $\Delta\sigma$, for $l = 1, 2, \dots, L$. We combine this two cost function together and becomes

$$S_{msc}(\lambda_r, \lambda_g, \lambda_b) = \frac{1}{K} \sum_{p \in \{r, g, b\}} \sum_{l=1}^L \sum_{k=1}^K \left(\frac{\bar{\rho}_k^{p, \sigma_{l,1}} - \bar{\rho}_k^{p, \sigma_{l,2}}}{\bar{\rho}_k^{p, \sigma_{l,2}} - \lambda_p} \right)^2 \cdot \exp \left\{ \frac{1}{3LK} \sum_{p \in \{r, g, b\}} \sum_{l=1}^L \sum_{k=1}^K \ln(\bar{\rho}_k^{p, \sigma_{l,2}} - \lambda_p)^2 \right\}.$$

With the aware of $\lambda = \mathbf{A}(1 - t(x))$, that is $\lambda_p = A_p(1 - t(x))$ for $p = r, g, b$, we can change the above equation by substituting $A_p(1 - t(x))$ for λ_p ,

$$S_{msc}(t_k) = \frac{1}{K} \sum_{p \in \{r, g, b\}} \sum_{l=1}^L \sum_{k=1}^K \left(\frac{\bar{\rho}_k^{p, \sigma_{l,1}} - \bar{\rho}_k^{p, \sigma_{l,2}}}{\bar{\rho}_k^{p, \sigma_{l,2}} - A_p(1 - t_k)} \right)^2$$

$$\cdot \exp \left\{ \frac{1}{3LK} \sum_{p \in \{r,g,b\}} \sum_{l=1}^L \sum_{k=1}^K \ln \left(\bar{\rho}_k^{p,\sigma_{l,2}} - A_p(1 - t_k) \right)^2 \right\}.$$

Where t_k is the same term as $t(x)$. We use this combined cost function to estimate the transmission t of each region. Fig. 3.4 shows a result of transmission map by applying this method.

By the hazy image degradation model, the hazy region has small transmission value since its intensity has a large portion comes from atmospheric light A instead of scene radiance J . We can use this idea to verify whether our transmission map is correct or not. We find that in Fig. 3.4, the transmission is darker in area which has denser fog as we predicted. The estimation of transmission map is overall correct.

We can see that the transmission map is not good enough. It may affect our final dehazing result and produce undesired artifacts. We want it to be more accurate and more sensitive to the edge discontinuities. So, we perform Soft Matting technique to refine our transmission map in order to reduce these annoying artifacts and get a better result. In the next subsection, we explain how we use Soft Matting method to refine this transmission map.



Fig. 3.4 The transmission map estimated by the cost function.

3.5 Refinement of Transmission Map using Soft Matting

The image matting equation is formed as following:

$$I(x) = \alpha(x)F(x) + (1 - \alpha(x))B(x),$$

where F is the foreground image, B is the background image and α is the pixel's foreground opacity. This equation is similar with the hazy image degradation model.

The transmission map is exactly the alpha map in image matting system. Thus, we decide to apply a soft matting method [4] to refine the transmission map estimated by the above subsection. Actually, we get this idea from Kaiming's work [13]. They also use this matting algorithm to refine their transmission map.

We transform the original cost function described in Soft Matting [4] into our

desired form:

$$E(t) = t^T L t + \lambda (t - \tilde{t})^T (t - \tilde{t}).$$

$t(x)$ is the refined transmission map and $\tilde{t}(x)$ is our transmission map produced by using the above cost function. L is the Matting Laplacian matrix proposed by Levin [4]

and λ is a regularization parameter. The (i, j) element of matrix L is defined as:

$$\sum_{k|(i,j) \in w_k} \left(\delta_{ij} - \frac{1}{|w_k|} (1 + (\mathbf{I}_i - \mu_k)^T \left(\Sigma_k + \frac{\varepsilon}{|w_k|} \mathbf{I}_3 \right)^{-1} (\mathbf{I}_j - \mu_k)) \right),$$

where \mathbf{I}_i and \mathbf{I}_j are the colors of the input image \mathbf{I} at pixels i and j , δ_{ij} is the Kronecker delta, μ_k and Σ_k are the mean and covariance matrix of the colors in window w_k , \mathbf{I}_3 is a 3×3 identity matrix, ε is a regularizing parameter, and $|w_k|$ is the number of pixels in the window w_k .

This optimal equation can be solved by the following sparse linear system proposed by [13]:

$$(L + \lambda U)t = \lambda \tilde{t}$$

where U is an identity matrix of the same size as L . And λ should be set to a small value such as 10^{-4} so that t is softly constrained by \tilde{t} . Fig. 3.5 is a resultant transmission map after processing soft matting algorithm. We can see that the refined transmission map is able to capture the sharp edge discontinuities and outline the profile of the objects.



Fig. 3.5 The transmission map after refinement using soft matting.

3.6 Recovering the Scene Radiance

After obtaining refined transmission map and atmospheric light vector, we can recover the scene radiance by the hazy image degradation model:

$$J(x) = \frac{I(x) - A}{t(x)} + A.$$

But, for some pixels, the transmission value might be close zero. This will cause the scene radiance J to be noisy among these pixels. Therefore, we restrict the transmission values of these pixels to a lower bound t_0 , which indicates that a small certain portion of haze are preserved in very dense haze regions. So, the equation will be modified as:

$$J(x) = \frac{I(x) - A}{\max(t(x), t_0)} + A.$$

We can set t_0 to a typical value 0.1. This value is extracted from a series of experiments [13]. Fig. 3.6 shows our final dehazed result.



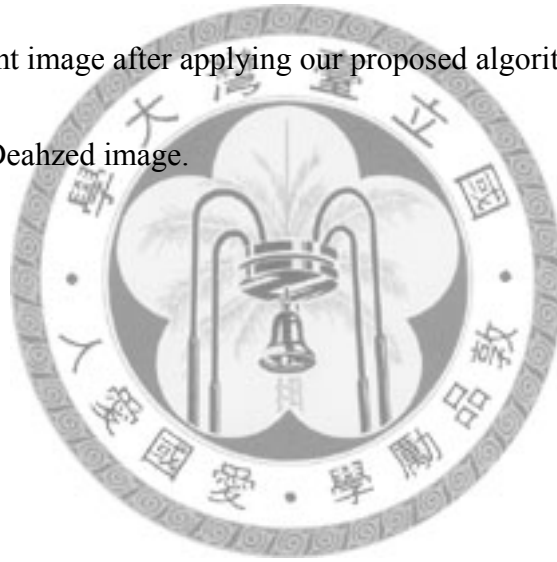
(a)



(b)

Fig. 3.6 The resultant image after applying our proposed algorithm.

(a) Input image. (b) Deahzed image.



Chapter 4 Experimental Results

We show the experimental results of the proposed system and comparisons with other haze removal methods in this chapter. In our proposed method, since we focus on recovering a haze-free image, we use a series of hazy images as our input images and recover haze-free images. Also, we compare the resultant images with other dehazing techniques to show the great outcome of our method.

4.1 Resultant images

The resultant images are presented in this subsection. We use images from others' papers [2][12][13], the Internet and some pictures taken by ourselves. We have some images of 300×300 and 600×400 as our input images. The comparisons with other dehazing methods are presented in the next subsection.

Figure 4.1 shows our haze removal result. 4.1(a) is the transmission map using the method proposed from section 3.4. We can see that the transmission map is not good enough. So, we apply the soft matting algorithm described in 3.5 to refine our transmission map as shown in Fig. 4.1(b). To compare with the original image, we put the input image and resultant image in 4.1(c) and 4.1(d). Clearly, the hazy layer of the image is removed and we can see the details of the flowers on the resultant image and

the red bricks become more lucid after processing our method.

Figure 4.2 shows another result. The transmission map shown in Fig.4.2(a) has some block-shaped regions; this is due to the mean shift segmentation. These blocks are segmented into regions since the varieties of these parts of the input image (shown in Fig. 4.2(c)) are very small. But after applying soft matting, this problem is well-solved. As can be seen in both results, our algorithm can recover vivid color information and unveil the details which are originally covered by haze.

In Figure 4.3(d), we can see that the input image (4.3(c)) becomes clearer and reveals more details after our dehazing procedure. Since the input image is too hazy to segment well, the transmission map (4.3(a)) doesn't look good. It contains sharp edges and block regions. After the refinement, the transmission map (4.3(b)) becomes great and solid for recovering scene radiance. Figure 4.4 also shows a result which its input image is taken from the sky like Fig. 4.3. The buildings and the vehicles become more lucid by our method.

Sometimes, when the transmission map is estimated well, we may not have to refine it. We can directly use it to recover the haze-free images. Figure 4.5 shows a result of this kind of transmission map. Despite the color inaccuracy of some area, the overall dehazing result seems satisfiable. This well-estimated transmission map comes from a well-segmented image. That is, once our input image is clear enough to segment

well, we may not have to exploit the matting method [4] to refine our transmission map.

Figure 4.6 through 4.9 are results using images taken by ourselves. Fig. 4.6(a) and 4.7(a) are images of city scenes taken from mountain areas. The results in Fig. 4.6(b) and 4.7(b) are well-dehazed and the city scenes become clearer. The mountains in Fig. 4.7(b) are clearer than they used to be in Fig. 4.7(a). Figure 4.8 shows a result of dust removal. The tiny rocks on the ground are vividly seen in the resultant image (4.8(b)) which are not and are covered by dust in the input image (4.8(a)). Figure 4.9 shows another result. The mountains and blue sign become more lucid. These results show that our method works well on real scene images.



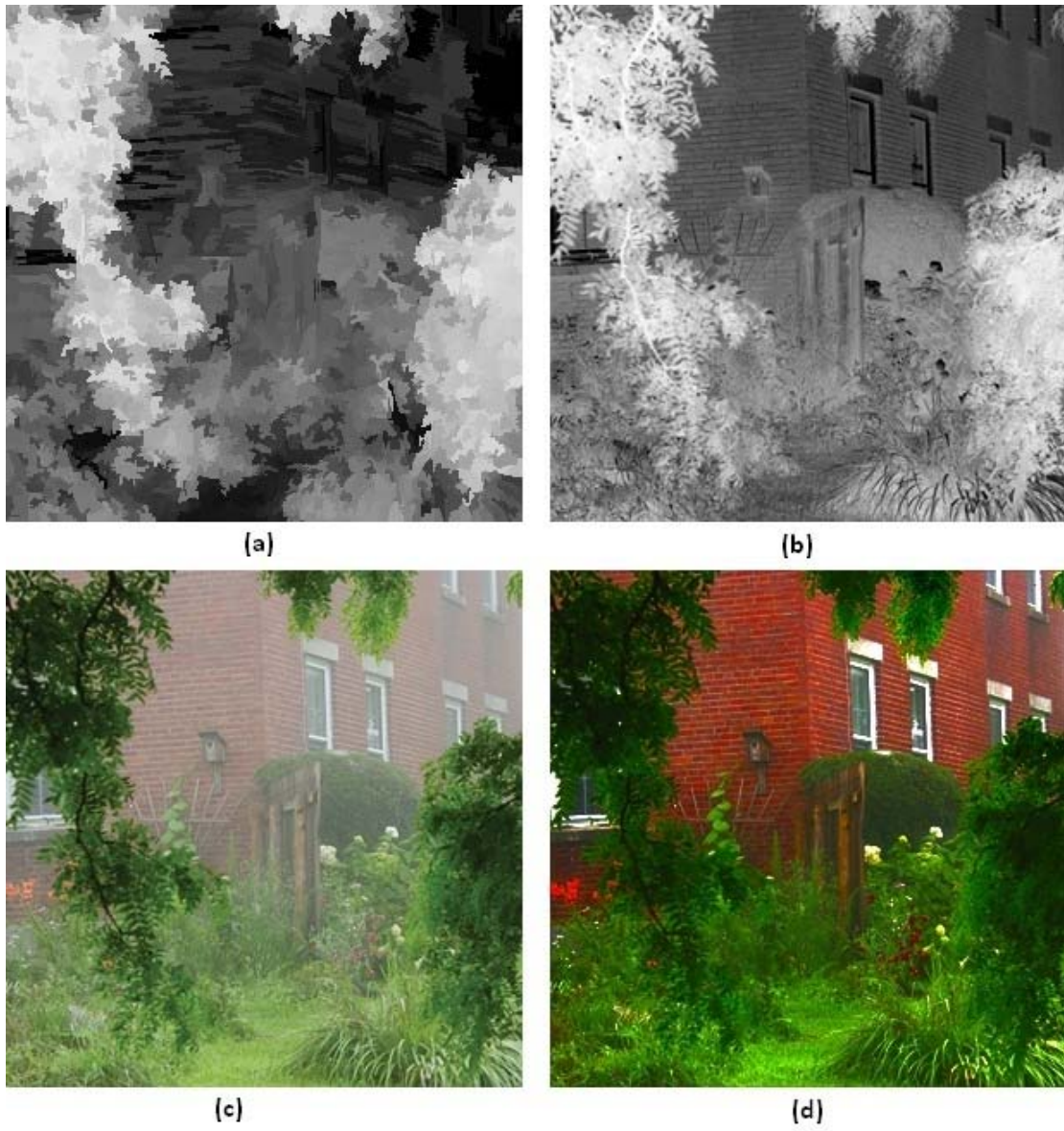


Fig. 4.1 A resultant image of our proposed haze removal method.

(a) Transmission map before refinement. (b) Transmission map after refinement.

(c) Input image. (d) Final dehazed image.

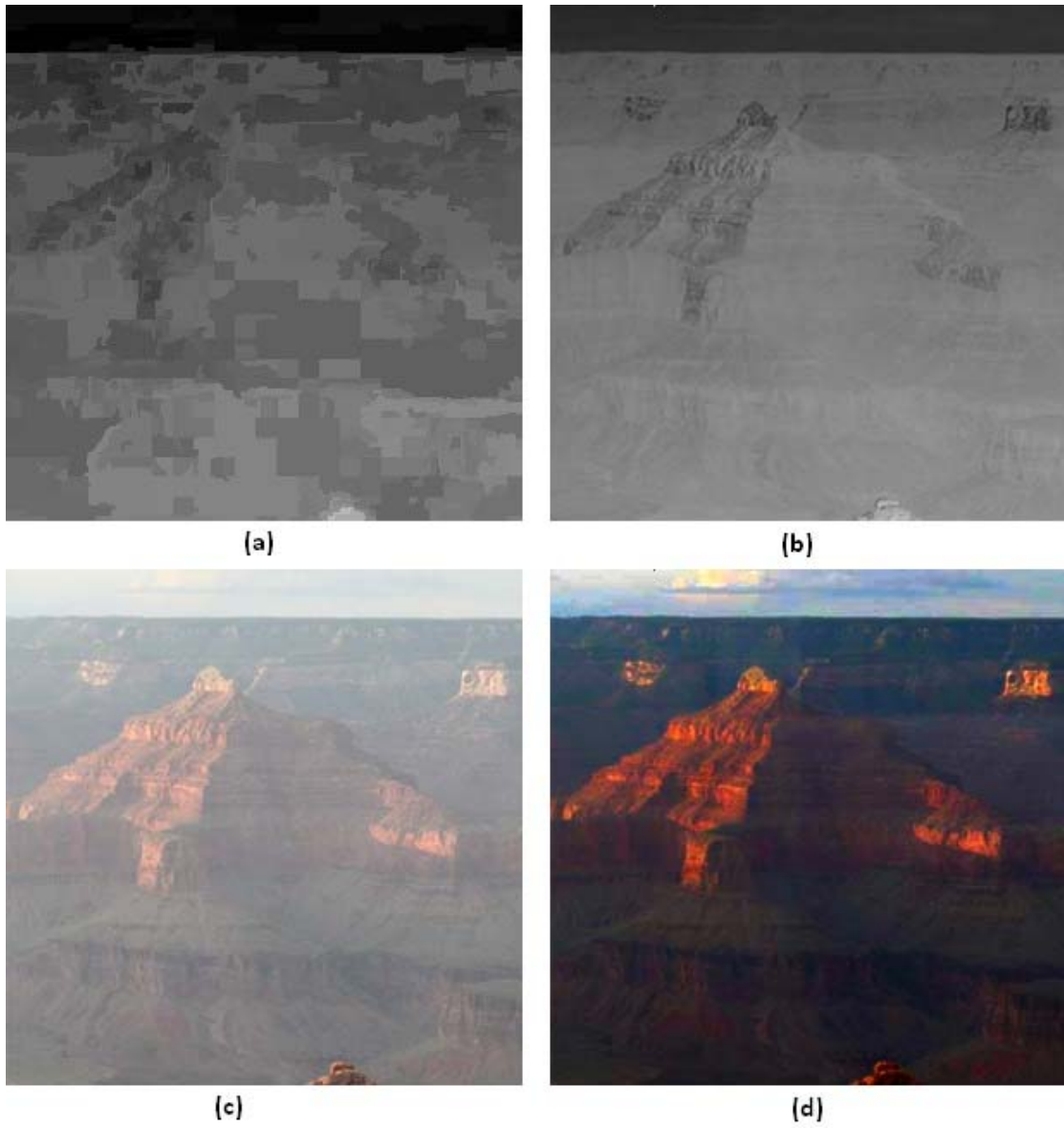


Fig. 4.2 A resultant image of our proposed haze removal method.

(a) Transmission map before refinement. (b) Transmission map after refinement.

(c) Input image. (d) Final dehazed image.

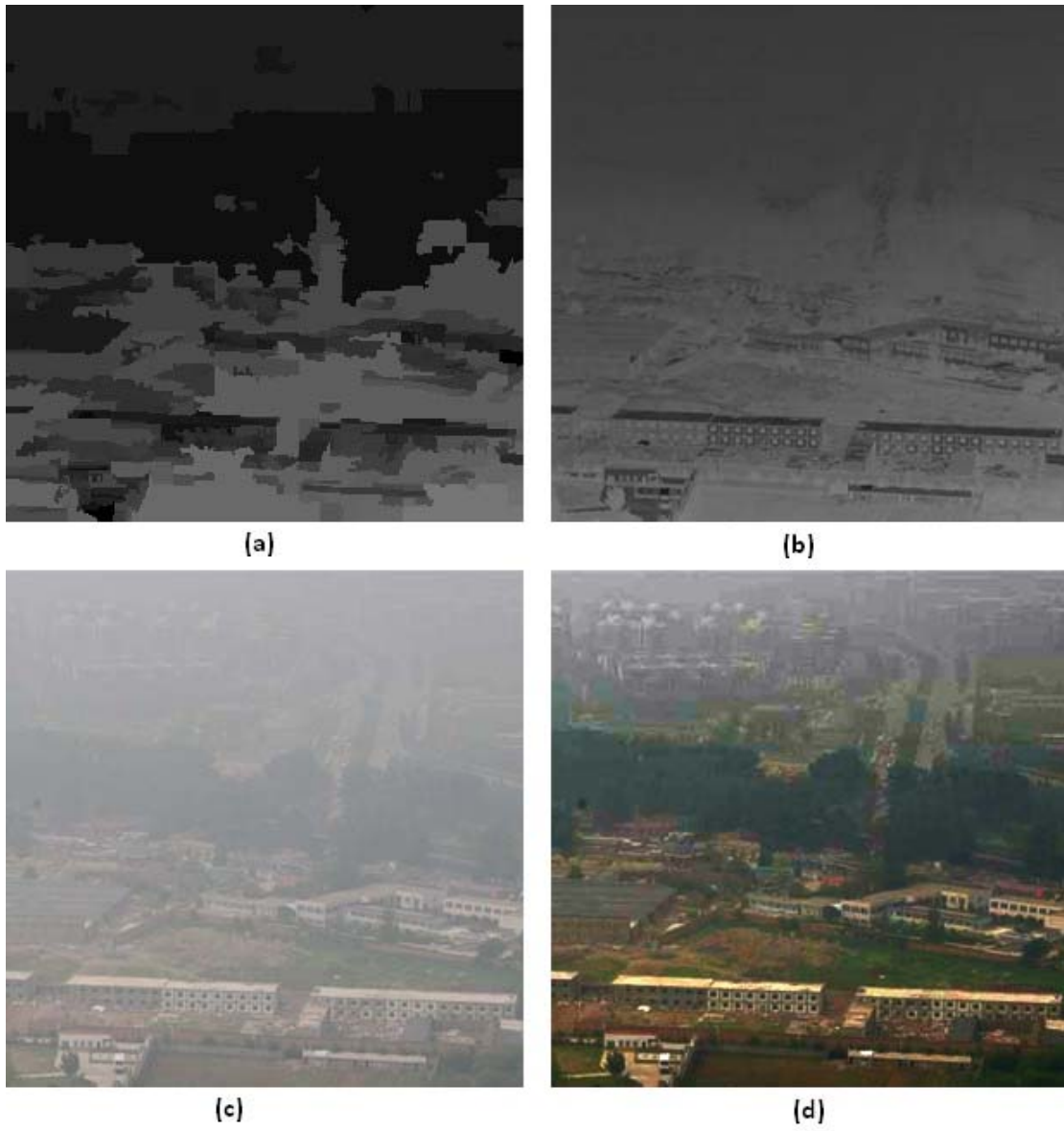


Fig. 4.3 A resultant image of our proposed haze removal method.

(a) Transmission map before refinement. (b) Transmission map after refinement.

(c) Input image. (d) Final dehazed image.

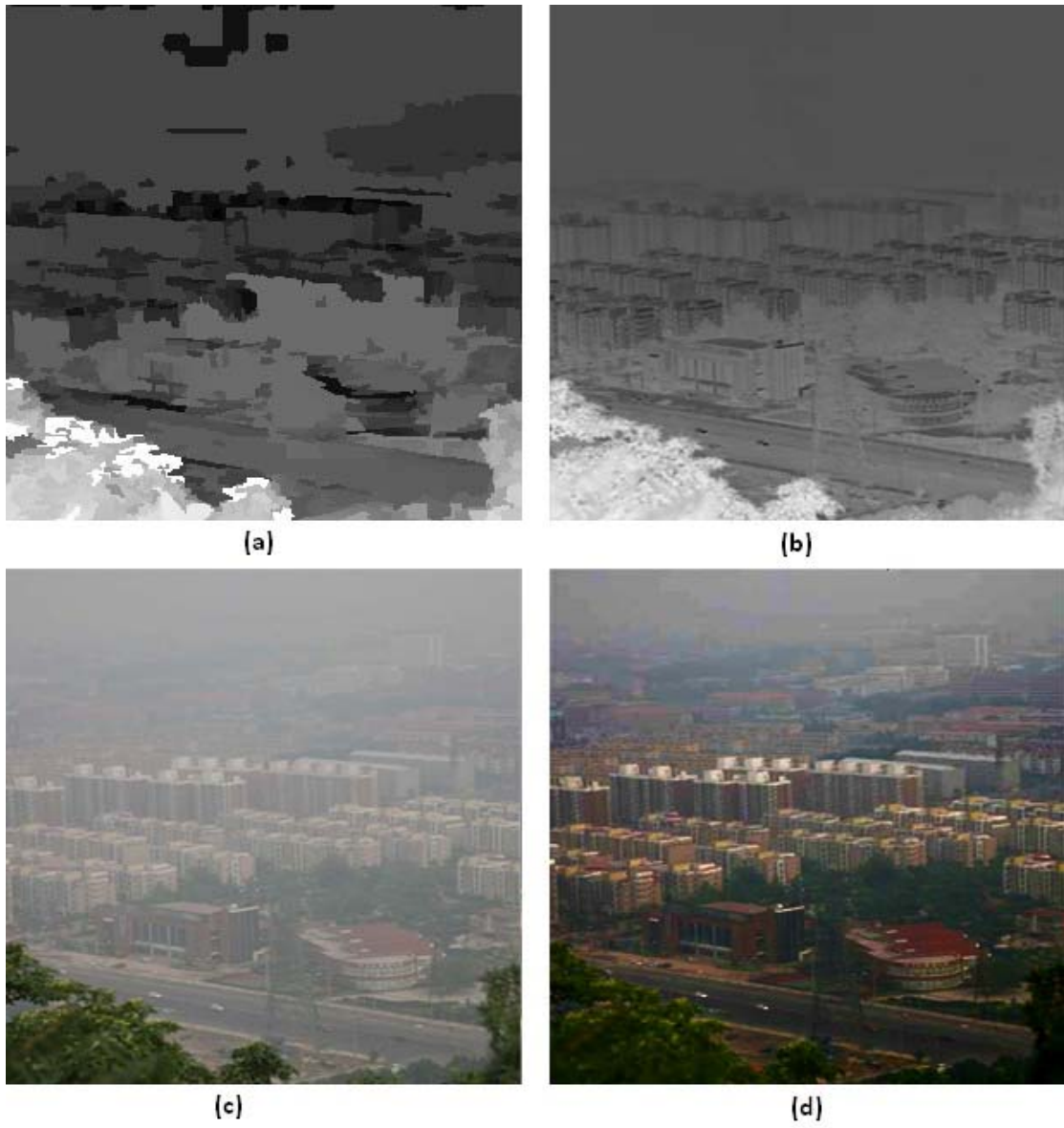


Fig. 4.4 A resultant image of our proposed haze removal method.

(a) Transmission map before refinement. (b) Transmission map after refinement.

(c) Input image. (d) Final dehazed image.

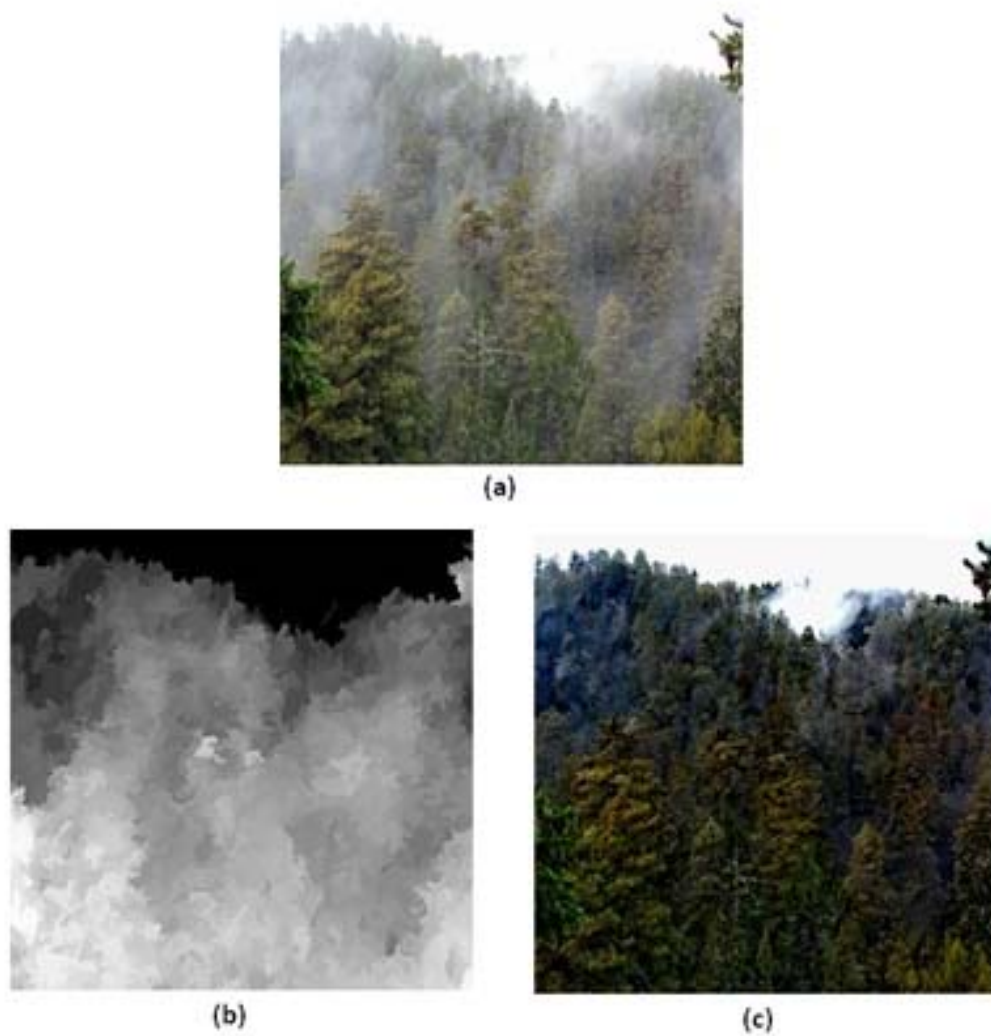


Fig. 4.5 Dehazing using the transmission map without refinement.

(a) Input image. (b) Unrefined transmission map. (c) Haze removal result.



(a)



(b)

Fig. 4.6 The resultant image from the image taken by ourselves.

(a) Input image. (b) Result.



Fig. 4.7 The resultant image from the image taken by ourselves.

(a) Input image. (b) Result.



(a)



(b)

Fig. 4.8 The resultant image from the image taken by ourselves.

(a) Input image. (b) Result.



(a)



(b)

Fig. 4.9 The resultant image from the image taken by ourselves.

(a) Input image. (b) Result.

4.2 Comparison with other haze removal methods

We compare our approach with Tan's method [12] in Figure 4.10. The resultant image of Tan's work shown in Fig. 4.10(b) looks abnormal and the color looks over saturated. This is because that their method is not physically based and may underestimate the transmission. Unlike their result, our result shows the right color and the appropriate amount of saturation. Also, Tan mentioned that his method produces halo artifacts in depth discontinuities. We don't have such issue in our resultant figures.

We also compare our approach with Dark Channel Prior method [13]. In Figure 4.11, we can see that their result is as good as our result since we both use soft matting method to refine our transmission map.

Figure 4.12 shows an comparison with Fattal's work [2]. Their work is based on statistics and need color information and variance to estimate the transmission. So, when their method encounters a dense haze layer or regions which are lacked for color variation, they fail to manage dehazing. Our method outperforms theirs in this circumstance as shown in Fig. 4.12(c). The mountain of their resultant image looks darker than our resultant image. Also, the roof of the building on the right side of the picture was transmission-underestimated in their result, but our result seems fine. Since our cost function can accurately find the transmission.

Our method performs well in haze removal. It outperforms several dehazing

approaches proposed recently. Our results reveal more details and can see clearly after haze is removed.

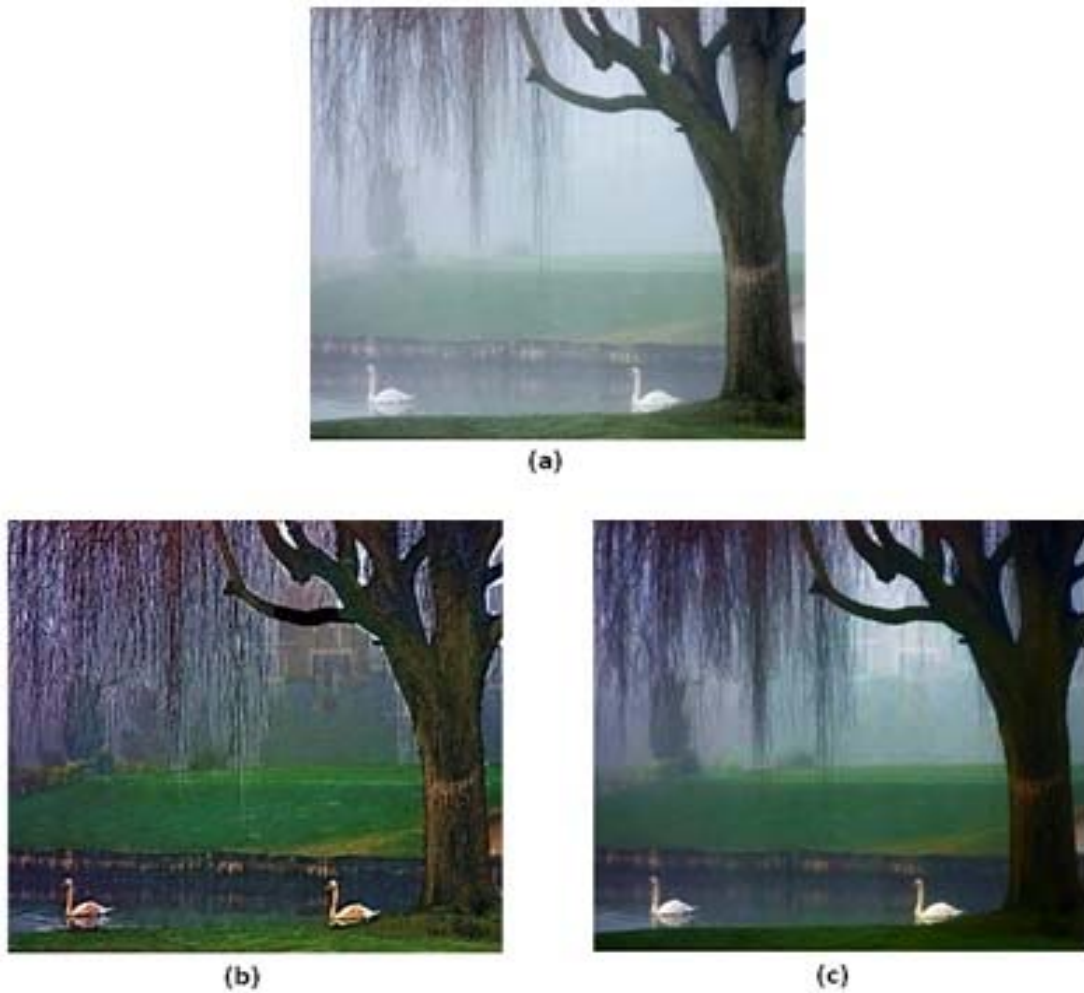


Fig. 4.10 Comparison with Tan's work [12].

(a) Input hazy image. (b) Tan's result. (c) Our result.

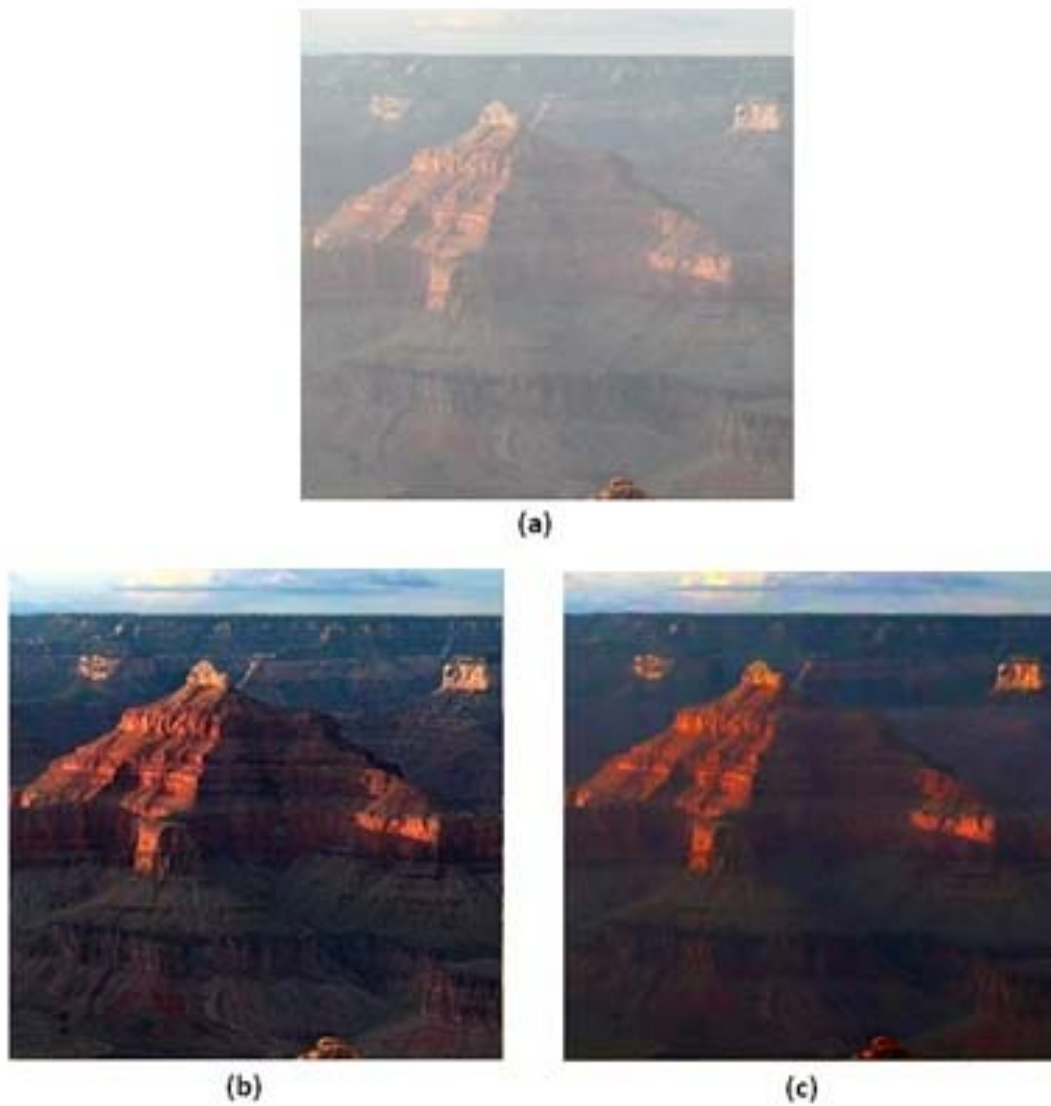


Fig. 4.11 Comparison with Dark Channel Prior method [13].

(a) Input hazy image. (b) Result of Dark Channel Prior method. (c) Our result.



(a)



(b)



(c)

Fig. 4.12 Comparison with Fattal's work [2].

(a) Hazy input image. (b) Fattal's result. (c) Our result.

Chapter 5 Conclusion and Future Work

5.1 Conclusions

In this thesis, we propose a content adaptive method for single image dehazing. We use a region segmentation algorithm to segment our input image into different regions. Then, by assuming pixels in each region have the same depth, we use the cost function we proposed to evaluate the transmission of each region. This cost function is based on the method proposed in [14].

We combine the multiscale and multichannel cost function together into a new cost function. After the transmission map is estimated by the cost function, image matting approach is then used to get a refined transmission map. Finally, a haze free image is recovered. This method is content adaptive since we use a segmentation method to classify our input into different group. We derive transmission of each group separately. The effectiveness of our proposed method can be seen in the previous section.

This method is based on image content and the observation that the depth of each region is the same. Even if the image is complex, we can use the mean segmentation to separate each region first and achieve haze removal. In addition, this dehazed image can be further exploited for advanced applications such as surveillance, smart vehicle and so on. Also, by the transmission map we estimated, the depth map of the scene can be

extrapolated.

5.2 Future work

Every method has its own limitations. In Tan's method [12], their resultant images have halos at depth continuities. In Fattal's method [2], it fails to remove haze when the haze in the image is dense. About our proposed method, when the input image contains a great portion of air, the radiance recovery step may not be done as well as other kind of images as shown in Figure 5.1. We think it's because that the transmission map is overestimated in those regions and causes an over-subtracting situation while recovering scene radiance. We think this overestimation is caused by our cost function. This is the problem we are going to deal with in the future. We intend to investigate this problem and renew our cost function in the future.

In Figure 5.2, the foreground of the image (a man and a woman riding horses) seems to be transmission-underestimated, but, the background is fine and is well-dehazed. For images like Fig. 5.2, we discover that we can use a detector to detect foreground and background first. Then, apply our method to the background and leave the foreground unchanged since our method performs well on background of this kind of images but underestimates the transmission in foreground. Face detection, Soft Matting are the detectors we think of recently. We think Soft Matting may perform the

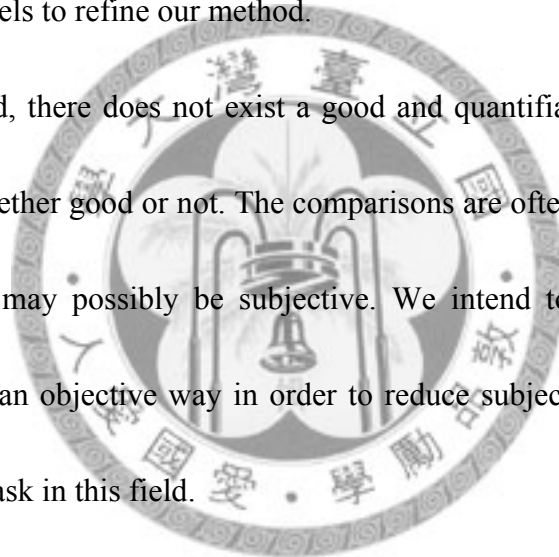
best since it is originally used to separate the background and foreground of an image.

We will implement this idea in the future.

Also, our work has another limitation that shares with most haze removal methods.

The common limitation is that the haze imaging model may be futile. We intend to study more appropriate models [13] for situations such as the sky regions affected by sun, and the blueish areas near the horizon. After studying the advanced models, we plan to use these models to refine our method.

In dehazing field, there does not exist a good and quantifiable way to effectively judge a method is whether good or not. The comparisons are often made by pure human sensitivity. So, they may possibly be subjective. We intend to figure out a way to compare methods in an objective way in order to reduce subjective comparisons. It is another challenging task in this field.



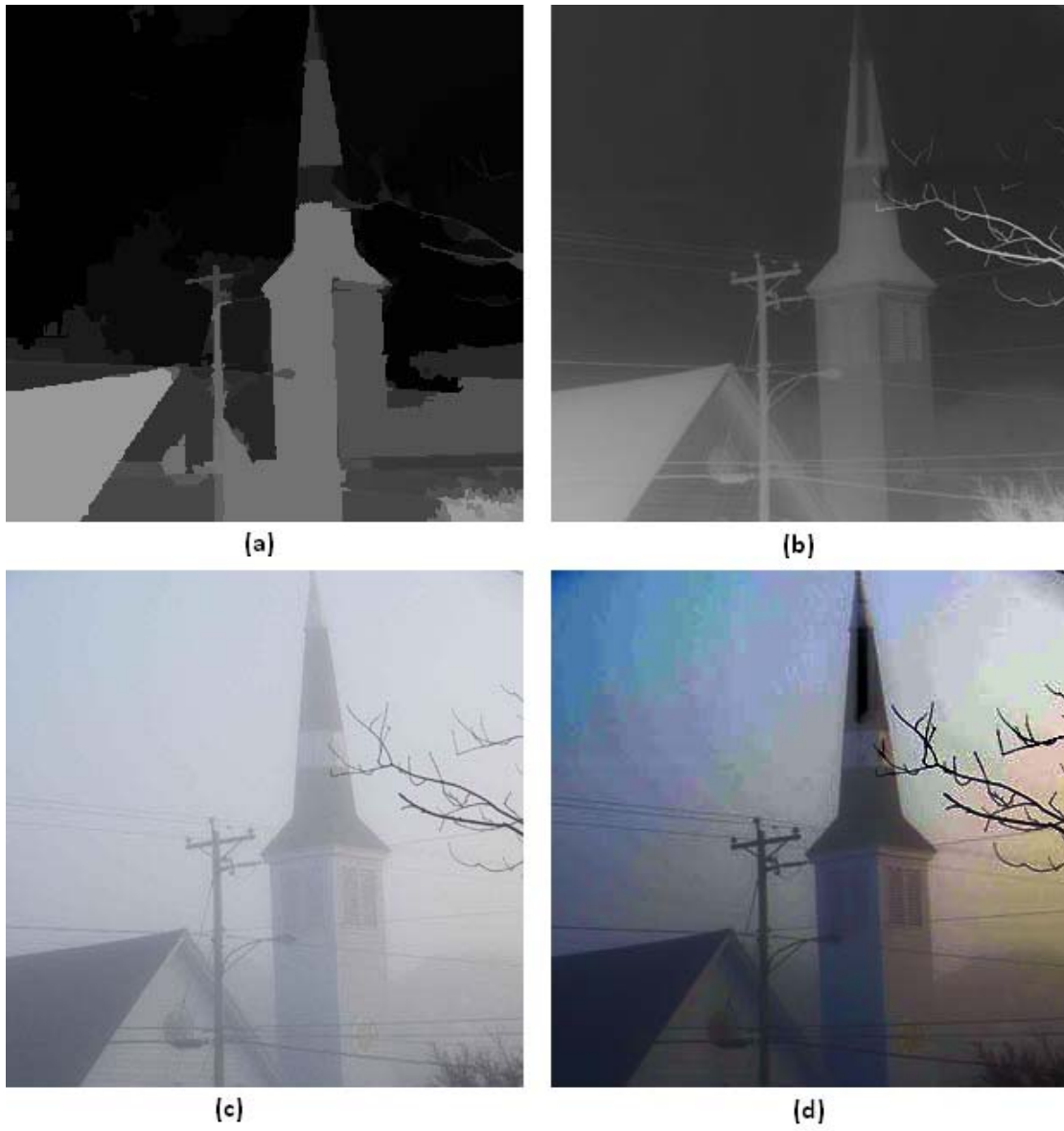


Fig. 5.1 Failure case. The image contains too much sky portion.

(a) Transmission map before refinement. (b) Transmission map after refinement.

(c) Input image. (d) Final dehazed image.



(a)



(b)

Fig. 5.2 Failure case from the image taken by ourselves.

(a) Input image. (b) Result.

REFERENCE

- [1] P. Chavez, “An improved dark-object subtraction technique for atmospheric scattering correction of multispectral data,” *Remote Sensing of Environment*, 24:450–479, 1988.
- [2] R. Fattal, “Single image dehazing,” *SIGGRAPH*, pages 1–9, 2008.
- [3] J. Kopf, B. Neubert, B. Chen, M. Cohen, D. Cohen-Or, O. Deussen, M. Uyttendaele, and D. Lischinski, “Deep photo: Model-based photograph enhancement and viewing,” *SIGGRAPH Asia*, 2008.
- [4] A. Levin, D. Lischinski, and Y. Weiss, “A closed form solution to natural image matting,” *CVPR*, 1:61–68, 2006.
- [5] S. G. Narasimhan and S. K. Nayar, “Chromatic framework for vision in bad weather,” *CVPR*, pages 598–605, 2000.
- [6] S. G. Narasimhan and S. K. Nayar, “Vision and the atmosphere,” *IJCV*, 48:233–254, 2002.
- [7] S. G. Narasimhan and S. K. Nayar, “Contrast restoration of weather degraded images,” *PAMI*, 25:713–724, 2003.
- [8] S. G. Narasimhan and S. K. Nayar, “Interactive deweathering of an image using physical models,” *Workshop on Color and Photometric Methods in Computer*

Vision, 2003.

- [9] S. K. Nayar and S. G. Narasimhan, “Vision in bad weather,” *ICCV*, page 820, 1999.
- [10] Y. Y. Schechner, S. G. Narasimhan, and S. K. Nayar, “Instant dehazing of images using polarization,” *CVPR*, 1:325, 2001.
- [11] S. Shwartz, E. Namer, and Y. Y. Schechner, “Blind haze separation,” *CVPR*, 2:1984–1991, 2006.
- [12] R. Tan, “Visibility in bad weather from a single image,” *CVPR*, 2008.
- [13] K. He, J. Sun and X. Tang, “Single Image Haze Removal Using Dark Channel Prior,” *CVPR*, 2009.
- [14] J. P. Oakley and H. Bu, “Correction of simple contrast loss in color images,” *IEEE Transactions on Image Processing* 16, 2, 511–522, 2007.
- [15] D. Comaniciu and P. Meer, “Mean shift: a robust approach toward feature space analysis,” *IEEE Transactions on Pattern Analysis and Machine Intelligence* Volume 24, Issue 5, Page(s):603 – 619, May 2002.
- [16] X. Chen, X. Yan and X. Chu, “Fast Algorithms for Foggy Image Enhancement Based on Convolution,” *International Symposium on Computational Intelligence and Design (ISCID)*, Volume 2, 17-Page(s):165 – 168, Oct. 2008.
- [17] D. Kim, C. Jeon, B. Kang and H. Ko, “Enhancement of Image Degraded by Fog

Using Cost Function Based on Human Visual Model,” *Multisensor Fusion and Integration for Intelligent Systems (MFI)*, Page(s):64 – 67, 20-22 Aug. 2008.

